First Observation of (100) and (211) Facets on ^{3}He Crystals

Raymond Wagner, Stephen C. Steel, Olga A. Andreeva,* Reyer Jochemsen, and Giorgio Frossati
Kamerlingh Onnes Laboratorium, Leiden University, P.O. Box 9506, 2300 RA Leiden, The Netherlands
(Received 29 August 1995)

Images of ^{3}He crystals at temperatures down to 1 mK have been obtained by means of a new type of optical cryostat, relying on the use of a compact charge-coupled device camera inside a nuclear demagnetization refrigerator. During growth from the superfluid ^{3}He-*A* phase, some crystals have shown second and third roughening, i.e., the presence of (100) and (211) facets in addition to the (110) facets previously observed. The presence of these new facets is in accordance with the Kosterlitz-Thouless theory of the roughening transition.

PACS numbers: 67.80.–s, 68.35.Rh, 81.10.Aj

The growth of crystals from their melt phase is, in general, accompanied by flows of mass and heat, which are due to the density and entropy differences between the two bulk phases. In ordinary systems, these diffusive transport processes limit the rate of solidification or melting for a given chemical potential difference $\Delta\mu$ applied across the crystal surface. The crystal dynamics are consequently very slow, giving rise to metastable rather than equilibrium crystal shapes.

In the case of helium crystals at low enough temperatures an unusual situation occurs. Because of the superfluid nature of the liquid, the high thermal conductivity of the solid, and the small latent heat of solidification, bulk transport properties no longer limit the velocity v of the crystal surface. Instead, v is determined by the interaction of the interface with the elementary excitations present in the bulk phases. Both theory [1] and experiment [2] have shown that the isothermal growth coefficient or intrinsic mobility k of ^{4}He crystals, defined by the relation $v = k\Delta\mu$, increases as T^{-4} at temperatures below 0.5 K. Consequently, ^{4}He crystals relax to their equilibrium shapes within milliseconds in this temperature region.

The experimental situation is more complicated for ^{3}He. As the superfluid transition of the liquid occurs at a temperature of only $T_A = 2.49$ mK, and the latent heat of solidification is more than a factor of 10^5 larger than that of ^{4}He at temperatures between 2.5 and 100 mK, one is again confronted with the bulk transport processes of mass and heat reducing the effective mobility of the crystal surface. In order to reach the regime where this mobility is determined by its intrinsic value, i.e., only by the interaction with the elementary excitations, one needs temperatures below the solid ordering temperature, $T_N = 0.93$ mK. In this temperature region the liquid is superfluid, and the latent heat decreases as T^4 [3].

Conventional optical cryostats contain several sets of windows, allowing the contents of the sample cell to be observed by an optical system outside the cryostat, operating at room temperature. Despite the use of infrared filters, these setups are currently limited to a sample temperature of 20 mK due to the thermal radiation entering the cryostat through the windows [4]. Therefore, they cannot be used to study the growth of ^{3}He crystals from the superfluid phase.

In this Letter, we present results obtained with an alternative type of optical cryostat, which houses the entire optical system inside its inner vacuum can. Thus, windows are required only in the sample cell. A charge-coupled device (CCD), operating at 65 K, is used as a camera. Because of the absence of windows in the cryostat and the low operating temperature of the camera, the heat leak on the sample cell is about 10 nW instead of the 10 μW typical of conventional optical cryostats. A similar optical cryostat, designed for interferrometric measurements, has been constructed by the Helsinki group [5]. The cryostat, optical system, and experimental cell are all as described in Ref. [6], except for the Cu nuclear demagnetization stage and Pt-NMR thermometer which were subsequently added. These improvements, described in Ref. [7], enabled us to obtain optical images of the nucleation of ^{3}He crystals from the superfluid *B* phase with stable temperatures down to $T = 0.8$ mK. The well-known melting pressure curve [8] was used to infer the temperature from the pressure measured in the cell. The Pt-NMR thermometer was used when there was no solid ^{3}He present and at temperatures below 1 mK, where it is more accurate than the melting curve thermometer.

The high mobility of helium crystal surfaces at low temperature has allowed the first quantitative experimental study of the roughening transition. This transition separates the atomically smooth surface state at low temperature from the atomically rough state at high temperature. According to theory [9,10], the roughening transition is of the Kosterlitz-Thouless type, and should occur at the roughening temperature T_R, given by

$$k_B T_R = \frac{2}{\pi}\,\gamma_R d^2, \tag{1}$$

with k_B Boltzmann's constant, γ_R the surface stiffness at T_R, and d the interplanar spacing, i.e., the distance between subsequent crystalline planes, measured in the direction normal to the crystal surface. The temperature

dependence of the surface stiffness has been calculated within the sine-Gordon model by renormalization of the interactions due to thermal fluctuations, giving [10]

$$\gamma(T) = \gamma_0\left[1 + t + \frac{1}{2}t_c - \sqrt{t(t + t_c)}\right], \quad (2)$$

with t the reduced temperature $(T - T_R)/T_R$, and t_c the so-called coupling strength, which is a measure of the pinning strength of the periodic lattice potential [11]. Well above the roughening temperature, the surface stiffness has the value γ_0. Near T_R it shows a cusp, reaching a value $\gamma_R = \gamma_0[1 + (1/2)t_c]$ at the transition temperature. Below T_R the surface stiffness is infinite.

As the interplanar spacing d in Eq. (1) is a function of the Miller indices of the crystal planes, each surface orientation will have a corresponding roughening temperature. Thus, on lowering the temperature, a sequence of roughening transitions is expected to occur on a crystal surface in equilibrium, giving rise to more and more macroscopically smooth facets. At $T = 0$, all orientations are predicted to be in the atomically smooth state [9], corresponding to a completely faceted crystal shape.

In helium, the coupling strength t_c is small [11]. As a result, the equilibrium size of a facet, which depends on t_c as $\exp(-\pi/2\sqrt{tt_c})$ according to the sine-Gordon model [10], is too small to allow a direct observation of the roughening transition on the equilibrium shape of a helium crystal.

In contrast to the equilibrium situation, facets can be quite large during crystal growth. An atomically smooth facet can grow only by the motion of steps and by the nucleation of new layers. The rough surfaces that surround each facet are able to grow as atoms stick independently to random sites, a process that is usually much faster. As the quickly growing rough surface at the edge of the slowly growing facet catches up, it is incorporated into the facet: the facet increases in size. Three roughening transitions on hcp ^{4}He crystals have thus been observed during crystal growth, at temperatures $T_{R1} = 1.30$ K, $T_{R2} \sim 1$ K, and $T_{R3} \sim 0.4$ K, in good agreement with Eq. (1) [2,12–15].

The sequence of images in Fig. 1 shows an example of the results we obtained on the growth of bcc ^{3}He crystals from the superfluid A phase. The circular light beam which is visible in the images has a diameter of 5 mm. The crystal is visible in the lower halves of the images. The rest of the cell contains liquid. The irregularities in the background and the black obstruction at the bottom of the images are artifacts of the optical system, and are not related to the contents of the sample cell. Image (a) shows the crystal while it is growing due to a compression of the sample cell volume. Faceted orientations grow markedly slower than rough orientations, resulting in a completely faceted growth shape. The lines visible within the crystal contour are the edges of the facets. The smaller facets can be difficult to discern against the background in a single image, but they are easily identified when viewed in an animated sequence of successive images. In image (b), the crystal has assumed a more rounded shape on melting (decompression). Resuming the compression results in a faceted growth shape again, shown in the third image (c).

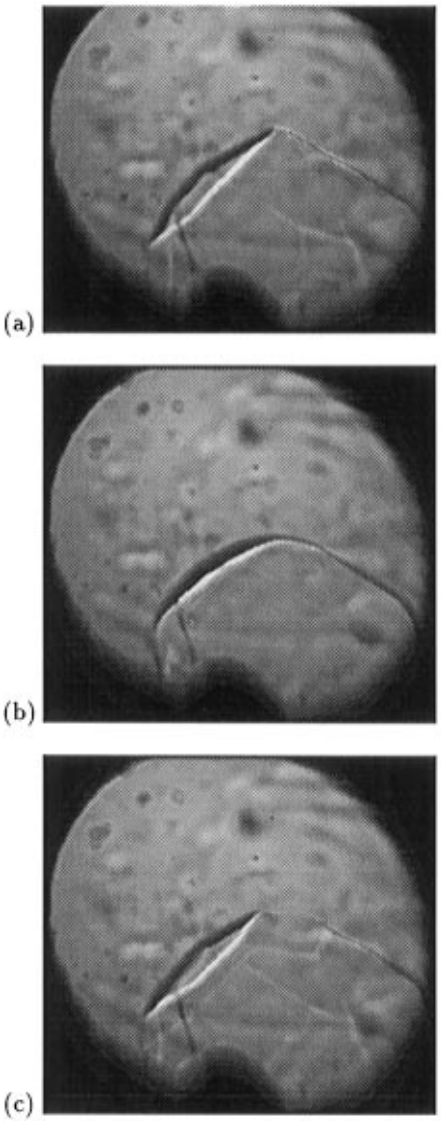

FIG. 1. Images of a ^{3}He crystal at a temperature of 2.2 mK while being grown (a), melted (b), and regrown (c). The relative sizes of the facets depend on the initial shape of the crystal before the growth is started.

In order to determine the type and orientation of the facets that are visible, it is helpful to know the order in which the facets should appear according to Eq. (1). Table I lists the orientations with the largest interplanar spacings d of the body-centered cubic lattice. Provided the temperature dependence and anisotropy of γ_R are small enough to be ignored, the roughening temperature should be expected to vary as d^2 according to Eq. (1), so the ratios $[d\,(110)/d\,(hkl)]^2$ are also listed in the table.

TABLE I. The five densest planes in the bcc lattice and their squared interplanar spacings relative to that of the (110) plane.

Miller indices (hkl)	$d^2(110)/d^2(hkl)$
(110)	1
(100)	2
(211)	3
(310)	5
(111)	6

We have simulated the observed two-dimensional projections of the crystals by means of a computer reconstruction. Each facet plane f_i is defined by the normal vector $\mathbf{r}_i$ extending from the origin to the plane. The edges of the facets are simply given by the intersections of all the planes f_i. A two-dimensional projection of these edges is constructed as a function of the projection direction $\hat{\mathbf{n}}$. The directions of the $\mathbf{r}_i$ are determined by their Miller indices, while the lengths of the $\mathbf{r}_i$ can be varied to change the size of the corresponding facet. The effect of a cell window can be represented by an additional plane with $\mathbf{r}_i$ parallel to $\hat{\mathbf{n}}$.

As a crystal grows, more facets become visible, as in Fig. 2(a). At this point it is possible to identify some of the facets, and thus determine the orientation of the crystal to a first approximation. The sizes of the facets can then be adjusted by varying the lengths of the vectors $\mathbf{r}_i$. This procedure is repeated until an orientation is found that is consistent with all the images taken during different stages of growth of a given crystal. In Fig. 2(b), the result of this procedure applied to image (a) is shown. It appears that most of the crystal surface consists of (110) facets. These facets have also been observed by Rolley, Balibar, and Gallet [16,17], and are indeed the first ones to be expected according to Table I. In addition, we have made the first observation of both (100) and (211) facets on ^{3}He crystals. These facets and their Miller indices are indicated in Fig. 2(b). From Table I it is clear that these types were indeed to be expected on the basis of their interplanar spacings. No dependence of the relative sizes of the facets on the growth speed or orientation could be determined. The sizes of the facets during crystal growth appear to be mainly determined by the shape of the crystal just before it starts growing. If a large portion of the surface has an orientation close to a facet direction, then a large facet will be produced. This can be seen in Fig. 1: The roughly horizontal top surface that forms when the crystal melts leads to the appearance of a much larger (001) facet when growth resumes.

Crystals nucleated from the superfluid B phase exhibited essentially the same behavior. Even at the lowest temperatures we were able to reach ($T = 0.8$ mK, just below the solid ordering transition T_N), we did not observe any evidence of a large increase in the crystal growth coefficient: When maintained in equilibrium conditions, the crystals did not show any sign of relaxing to their equilibrium shape on the time scale of our observations (several hours).

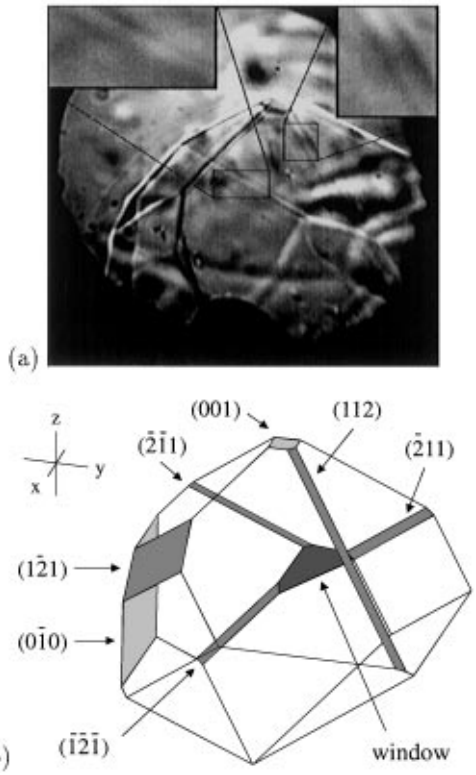

FIG. 2. (a) Image of the same crystal as shown in Fig. 1, during a later stage of its growth. In order to improve the visibility of the faint (112), $(\bar{2}\bar{1}1)$, and $(\bar{1}\bar{2}\bar{2})$ facets, the contrast relative to an image without a crystal present has been increased [20]. (b) Computer reconstruction of the crystal shown in (a), with Miller indices of the observed (100) and (211) facets indicated. The unshaded planes are (110) facets.

We conclude with some remarks about the roughening temperatures corresponding to the (100) and (211) orientations. The surface stiffness of ^{3}He crystals has been determined from equilibrium shape measurements made at the melting curve minimum ($T_m = 316$ mK): $\gamma(T_m) = 60 \pm 11\ \mu\mathrm{J\,m^{-2}}$ [18]. If we treat this value as the high temperature limit γ_0, then $\gamma_R = (1 + t_c/2)\gamma(T_m)$. As an estimate for an upper limit on t_c, we can take the value found for ^{4}He crystal surfaces oriented perpendicular to the sixfold symmetry axis, $t_c = 0.6$ [19]. We would expect t_c to be lower than this in ^{3}He because of the larger zero point motion of the atoms [11]. Assuming t_c lies in the range $0 < t_c < 0.6$, we can use Eq. (1) to estimate T_R for various facets: $T_R(110) \sim 260$–340 mK, $T_R(100) \sim 130$–170 mK, and $T_R(211) \sim 87$–113 mK.

We now recall the results obtained by Rolley, Balibar, and Gallet [16,17] who observed (110) facets only below 100 mK, and no other types down to 60 mK. This

discrepancy was explained by the theory of dynamic roughening, which states that in the presence of an applied chemical potential difference across the interface (which is always present during crystal growth) the roughening transition is broadened and displaced to a lower temperature [10,19]. This displacement is larger for larger $\Delta\mu$ and smaller t_c. The (110) facets were observed only below a temperature of roughly $T_R/3$. If we assume that we grow our crystals at a similar $\Delta\mu$, and that the reduction of the roughening temperature is isotropic, then the (100) and (211) transitions are expected near 50 and 35 mK, respectively.

It would be very interesting to measure the temperatures at which the (100) and (211) facets actually appear. However, when the sample is heated above the superfluid transition temperature, the experimental study of ^{3}He crystal growth becomes very difficult. Because of the finite thermal conductivity, unwanted thermal gradients are easily set up in the cell. For instance, dust specks on the windows can absorb light and locally warm up the liquid. In addition, due to the Pomeranchuk effect the liquid near the growing crystal can become colder than elsewhere in the cell. Consequently, there is a high probability of nucleating new ^{3}He crystals at the warmest spots elsewhere in the sample cell, particularly when high compression rates are used. Quite often several crystals will touch each other during growth, or they will grow in regions of the cell that are invisible to the optical system. As a result, we saw no evidence for facet types other than (110) at temperatures above 2.5 mK. The best chance of observing these facets might be obtained through the use of a cell which can be tilted at low temperature. The initially rounded crystal can then be rotated in such a way that a large part of its surface is lined up with the expected facet orientation before growth is initiated, analogous to what was seen in Figs. 1(b) and 1(c).

In summary, we have used a new type of optical cryostat for the study of growth shapes of ^{3}He crystals from the superfluid *A* phase. We have found evidence for the presence of (110), (100), and (211) facets on these growth shapes, the last two of which had never been observed in earlier studies. The three types of facets we observed are the three types predicted to be most stable according to the Kosterlitz-Thouless theory of roughening. A more quantitative study of the roughening temperatures and facet mobilities in various crystalline orientations should provide more information about the coupling strength t_c in the case of ^{3}He.

We thank C. M. C. M. van Woerkens for the construction of the pressure gauge, P. Remeijer and P. J. Ras for their assistance during several experiments, and A. V. Babkin and S. Balibar for useful discussions. This work was part of the research program of the Stichting voor Fundamenteel Onderzoek der Materie (FOM), which is financially supported by the Nederlandse Organisatie voor Wetenschappelijk Onderzoek (NWO).

*Permanent address: Kapitza Institute for Physical Problems, ul. Kosygina 2, 117334 Moscow, Russia.

[1] A. F. Andreev and A. Ya. Parshin, Zh. Eksp. Teor. Fiz. **75**, 1511 (1978) [Sov. Phys. JETP **48**, 763 (1978)].
[2] K. O. Keshishev, A. Ya. Parshin, and A. V. Babkin, Zh. Eksp. Teor. Fiz. **80**, 716 (1981) [Sov. Phys. JETP **53**, 362 (1981)].
[3] D. D. Osheroff and C. Yu, Phys. Lett. A **77A**, 458 (1980).
[4] E. Rolley, C. Guthmann, E. Chevalier, and S. Balibar, J. Low Temp. Phys. **99**, 851 (1995).
[5] J. P. Ruutu, H. Alles, A. V. Babkin, P. J. Hakonen, and E. Sonin, Europhys. Lett. **28**, 163 (1994).
[6] R. Wagner, P. J. Ras, P. Remeijer, S. C. Steel, and G. Frossati, J. Low Temp. Phys. **95**, 715 (1994).
[7] R. Wagner, S. C. Steel, O. A. Andreeva, A. N. Marchenkov, R. Jochemsen, and G. Frossati, J. Low Temp. Phys. **101**, 287 (1995).
[8] D. S. Greywall, Phys. Rev. B **33**, 7520 (1986).
[9] D. S. Fisher and J. D. Weeks, Phys. Rev. Lett. **50**, 1077 (1983).
[10] P. Nozières and F. Gallet, J. Phys. (Paris) **48**, 353 (1987).
[11] S. Balibar, F. Gallet, F. Graner, C. Guthmann, and E. Rolley, Physica (Amsterdam) **169B**, 209 (1991).
[12] J. E. Avron, L. S. Balfour, C. G. Kuper, J. Landau, S. G. Lipson, and L. S. Schulman, Phys. Rev. Lett. **45**, 814 (1980).
[13] S. Balibar and B. Castaing, J. Phys. (Paris), Lett. **41**, L329 (1980).
[14] P. E. Wolf, S. Balibar, and F. Gallet, Phys. Rev. Lett. **51**, 1366 (1983).
[15] O. A. Andreeva and K. O. Keshishev, Pis'ma Zh. Eksp. Teor. Fiz. **52**, 799 (1990) [JETP Lett. **52**, 164 (1990)].
[16] E. Rolley, S. Balibar, and F. Gallet, Europhys. Lett. **2**, 247 (1986).
[17] E. Rolley, S. Balibar, and F. Gallet, Jpn. J. Appl. Phys. **26**, Suppl. 26-3, 391 (1987).
[18] E. Rolley, S. Balibar, F. Gallet, F. Graner, and C. Guthmann, Europhys. Lett. **8**, 523 (1989).
[19] F. Gallet, P. Nozières, S. Balibar, and E. Rolley, Europhys. Lett. **2**, 701 (1986).
[20] The original digital images are available via WWW: "http://qv3pluto.LeidenUniv.nl/he3grow/".